

Mechanisms of the PtCl₂-Catalyzed Intramolecular Cyclization of *o*-Isopropyl-Substituted Aryl Alkynes for the Synthesis of Indenes and Comparison of Three sp³ C–H Bond Activation Modes

Yi Wang,^{†,§} Wei Liao,^{†,§} Genping Huang,[‡] Yuanzhi Xia,[‡] and Zhi-Xiang Yu^{*,†}

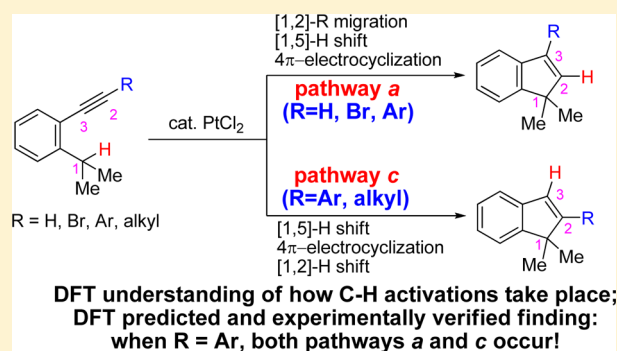
[†]Beijing National Laboratory for Molecular Sciences (BNLMS), Key Laboratory of Bioorganic Chemistry and Molecular Engineering of Ministry of Education, College of Chemistry, Peking University, Beijing 100871, China

[‡]College of Chemistry and Materials Engineering, Wenzhou University, Wenzhou, Zhejiang Province 325035, China

S Supporting Information

ABSTRACT: Chatani and He respectively reported an efficient way to synthesize indenes through PtCl₂ catalyzed sp³ C–H bond activation. Interestingly, the R group (R = H or Br) in the alkyne moiety of the substrates in Chatani's experiments migrates to the C3 position in indenes, whereas the R group (R = Ar) stays in the original C2 position of final indenes in He's experiments. DFT calculations indicated that there are two competing pathways *a* and *c* for the cyclization reaction. Pathway *a* involves [1,2]-R migration, [1,5]-H shift, and 4π-electrocyclization, giving the indenes with the R group at the C3 position. Pathway *c* takes place through irreversible [1,5]-H shift/cyclization and [1,2]-H shift, generating indenes with the R group at the C2 position. DFT calculations found that, when R = H or Br, pathway *a* is favored.

When R = alkyl group, the [1,2]-R migration is difficult and pathway *c* is preferred. When R = Ar, DFT calculations predicted and experiments verified that both pathways *a* and *c* occur to give two indene products. Comparison of different models of sp³ C–H activations has been presented to guide further understanding and prediction of new C–H bond activations.

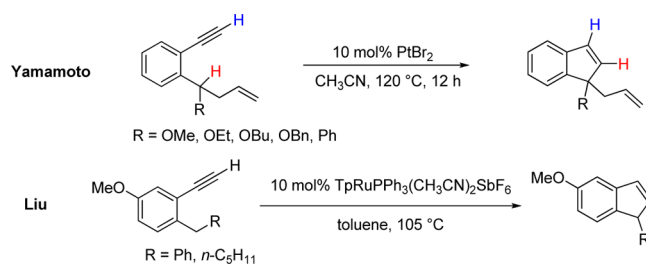


INTRODUCTION

Designing, discovering, and developing new C–H bond functionalization reactions is one of the most intensively investigated research fields in today's science of synthesis.¹ Understanding the mechanisms of the reported C–H bond functionalization reactions is very critical for advancing the related field, considering that the mechanistic insights obtained experimentally and/or computationally can provide useful hints and guidance for optimizing and developing new reactions and catalysts.² Unfortunately, even though many elegant C–H functionalization reactions have been developed, only a small number of these reactions have been investigated mechanistically.³ For example, recently, Yamamoto,⁴ Liu,⁵ Chatani,⁶ and He⁷ made great contributions in the field of the sp³ C–H functionalization (Schemes 1 and 2),⁸ but mechanistic understandings of how these reactions take place and what factors affect their different reactivity and regiochemistry have not been well studied.⁹ Herein, we report our DFT and experimental investigations of the mechanisms and regiochemistry of these PtCl₂-catalyzed C–H functionalization reactions.

In 2006, Yamamoto reported the PtBr₂-catalyzed cyclization reaction of 1-ethynyl-2-(1-alkoxybut-3-enyl)benzenes, giving functionalized indenes (Scheme 1).⁴ However, simple alkyl substituted compounds without methoxy groups were inapplicable even at high temperature (120 °C). Liu found that the

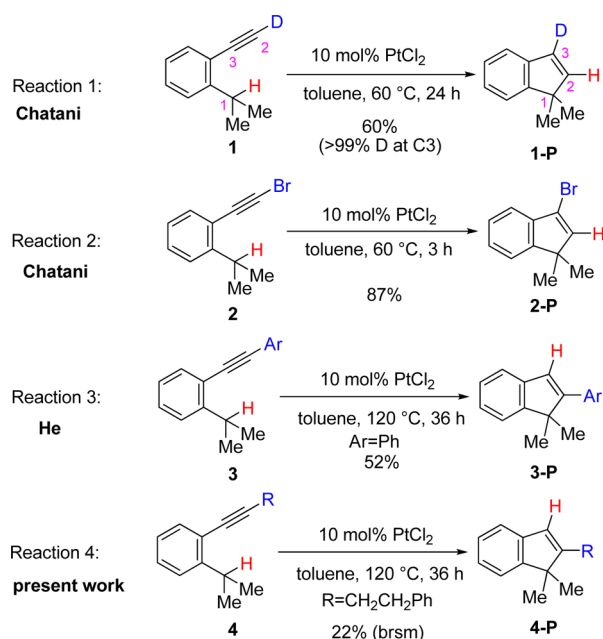
Scheme 1. Cyclization of Terminal Alkynes Reported by Yamamoto⁴ and Liu⁵



similar reaction can also be catalyzed by Ru catalyst (Scheme 1).⁵ Recently, Chatani's group and He's group independently made significant advances in this field (reactions 1–3, Scheme 2). Chatani and co-workers⁶ found that PtCl₂, PtCl₄, or [RuCl₂(CO)₃]₂ can serve as the general catalyst for the cyclization of 1-alkyl-2-ethynylbenzenes under relatively mild conditions (30–80 °C), leading to benzylic C–H bond functionalization products. It was demonstrated for the first time that simple tertiary C–H bonds can participate in this type of catalytic cyclization reaction to form all-carbon quaternary

Received: April 14, 2014

Published: April 30, 2014

Scheme 2. Cyclization Reactions Reported by Chatani Group⁶ and He Group⁷

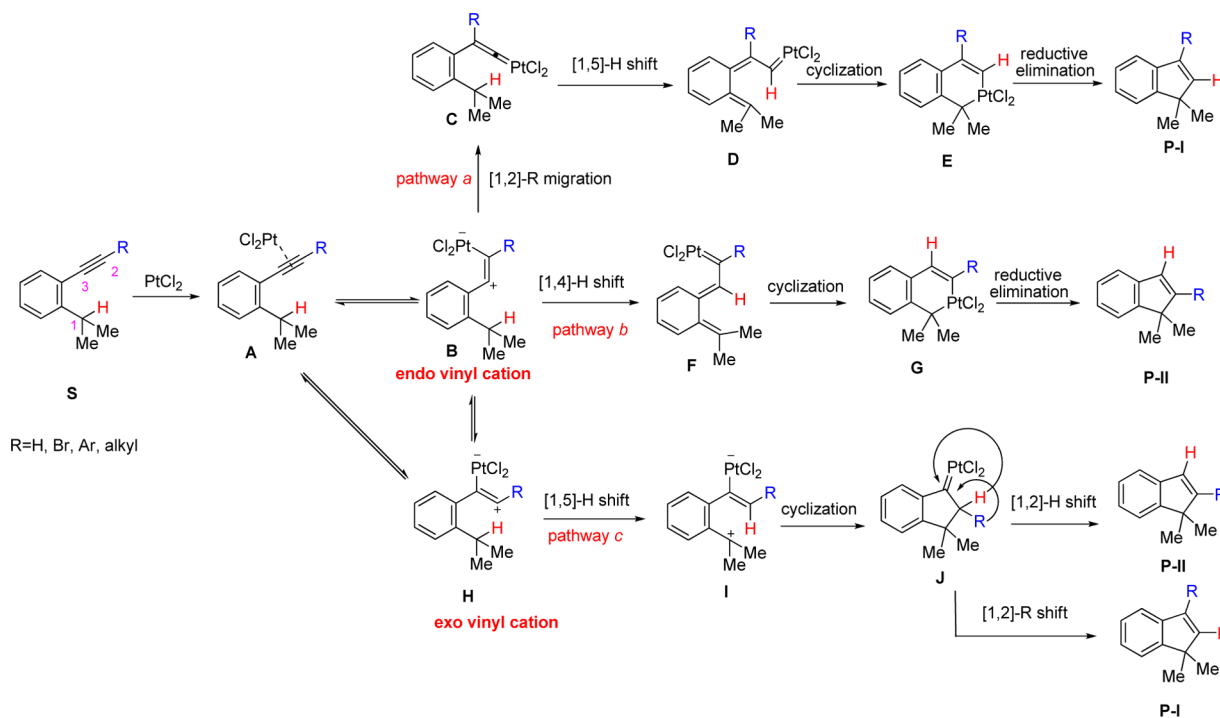
centers. They carried out some preliminary mechanistic investigations using deuterated alkyne **1** and Br-substituted alkyne **2** as the substrates and found that the deuterium atom and Br atom were selectively incorporated at the C3 position exclusively in the indene products **1-P** and **2-P**, respectively (reactions 1 and 2). He and co-workers later on found that the substituent in the alkyne part can be an aryl group, but the aryl group was incorporated at the C2 position of the final products (Scheme 2). This reaction's yield was 52%, but 82% it can be

reached if both PtCl_2 and CuBr were used as catalysts (see their original report for details).⁷

To our surprise, the proposed mechanisms for reactions 1–3 by Chatani and He are quite different (pathways *a* and *b*, Scheme 3). Chatani⁶ proposed that, for substrate **S** with $\text{R} = \text{H}$ or Br , the cyclization reaction starts from coordination of PtCl_2 to the triple bond in **S**, leading to the formation of $\text{Pt}-\pi$ -alkyne complex **A**, which can be viewed as an equilibrium structure of zwitterionic **B** (We name this equilibrium form as an endo vinyl cation, which is opposite to another equilibrium form, the exo vinyl cation **H**. Also **B** and **H** can be regarded as carbene species).¹⁰ Subsequently, the hydrogen or bromine at the terminal alkyne migrates to the adjacent internal β -carbon to form a vinylidene platinum intermediate **C**,¹¹ which activates the sp^3 C–H bond at the benzylic carbon. A [1,5]-H shift transforms the platinum vinylidene **C** into a Pt -carbene complex **D**. Complex **D** can be viewed as a metallocene, which then undergoes electrocyclic to form metallacycle **E**. Subsequent reductive elimination from **E** gives the final product **P-I**. Because of the existence of [1,2]-R migration, the migrated R (H or Br) was incorporated at the C3 position in the final indene products.

In contrast, He⁷ proposed a mechanism without [1,2]-R shifts for substrates with $\text{R} = \text{Ar}$ and alkyl groups (pathway *b*). In pathway *b*, complex **B**, an endo vinyl cation, undergoes a [1,4]-H shift to give Pt -carbene complex **F**, which then furnishes product **P-II** through cyclization and reductive elimination. In **P-II**, the R group is incorporated at the C2 position of the indene product.

We were very curious to know why different substrates have different reaction pathways. In addition, we proposed that there is another possible pathway, pathway *c* involving [1,5]-H shift/cyclization and [1,2]-R migration (H or R migration), to account for the experimental results from both Chatani and He

Scheme 3. Three Possible Pathways for PtCl_2 -Catalyzed Cyclization of Alkynes Proposed by Chatani (Pathway *a*),⁶ He (Pathway *b*),⁷ and Us (Pathway *c*)

groups. In pathway *c*, the PtCl₂–alkyne complex can be viewed as an exo vinyl cation species **H**, which can undergo [1,5]-H shift to give Complex **I**. Complex **I** then undergoes cyclization and [1,2]-H shift or [1,2]-R shift, generating indene products **P-II** or **P-I**, respectively.

Among the three possible pathways, three modes of C–H activations were involved from complexes **C**, **B**, and **H**, respectively (see also Scheme 4 in the later discussion). The

Scheme 4. DFT Computed Activation Free Energies (kcal/mol) for [1,2]-R Migration and C–H Activations in the Gas Phase

R	[1,2]-R migration	Three modes of C-H activations		
		pathway a	pathway b	pathway c
H	18.6	5.2	30.2	20.7
Br	15.9	3.8	25.0	20.4
Ph	19.7	5.8	30.2	17.7
Me	31.6	3.8	31.3	21.5

C–H bond is activated through [1,5]-H shift reaction from **C** in pathway *a* and **H** in pathway *c*, while in pathway *b*, the C–H bond is activated through the [1,4]-H shift from **B**. The activation free energies of three modes will be calculated and

compared so that this information can be helpful for the future design of C–H activation reactions.

In the present paper, we report our DFT study of the energy surfaces of the proposed pathways *a–c* for substrates with R = H, Br, Ph, and Me. Previously, Zhao and co-workers discussed several possible pathways of the indene formation from substrate with R = H.⁹ We aim here to answer which pathway, for a specific substrate, will be favored and the reason for this preference. We also tried to analyze the detailed potential energy surfaces for all these substrates to get the kinetic and thermodynamic data of these reactions and the structures of key transition states and intermediates. When calculation results were different from experiments, new experimental tests were carried out to support or disprove calculation results. In addition, we designed and studied reaction 4 (Scheme 2) computational and experimentally to understand how a substrate with an alkyl group in its alkyne part undergoes the C–H activation reaction using PtCl₂ as the catalyst.

COMPUTATIONAL METHODS

All calculations were performed with the Gaussian 09 program.¹² Density functional theory (DFT)¹³ calculations using the B3LYP functional¹⁴ were used to locate all the stationary points involved. The 6-31G(d) basis set¹⁵ was applied for all elements except for Pt, for which the LANL2DZ¹⁶ basis set and pseudopotential were used. This approach has been successfully applied to study structures and reaction mechanisms for reactions of PtCl₂ complexes and other Pt-catalyzed cycloadditions.¹⁷ Frequency calculations at the same level were performed to confirm each stationary point to be either a minimum or a transition structure. Intrinsic reaction coordinate (IRC)¹⁸ calculations were performed to confirm the connection of each transition state to its corresponding reactant and product. The single point energies were calculated by the M06¹⁹ method using the same basis set to include the contribution of dispersion energies (we found that in the present system, B3LYP and M06 gave very similar

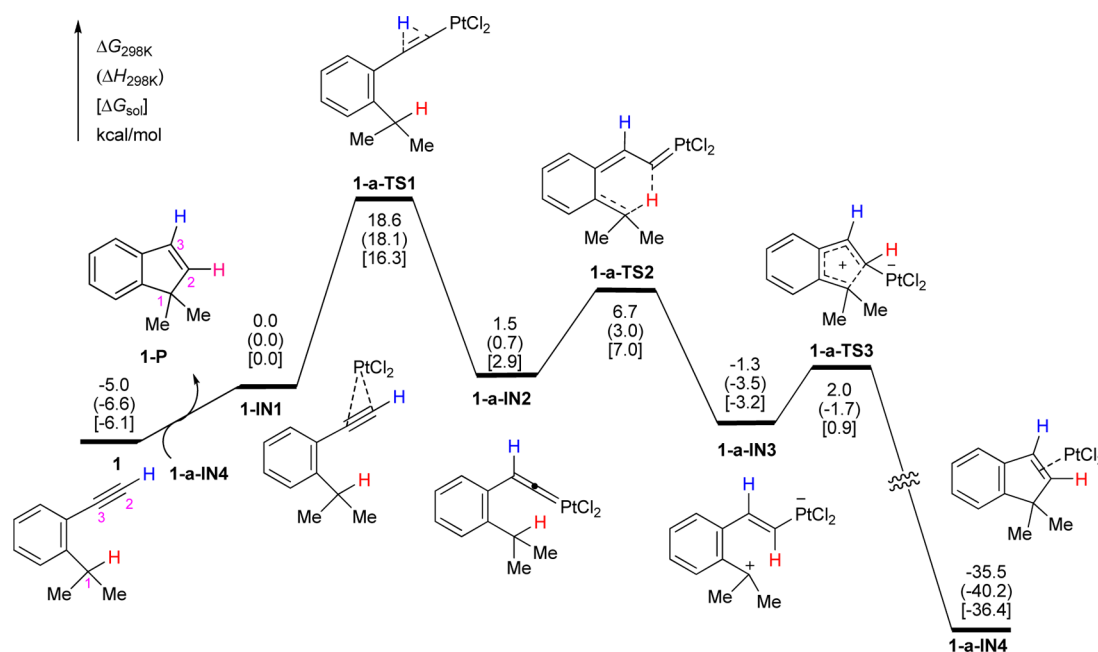


Figure 1. DFT computed energy surface of pathway *a* for the PtCl₂-catalyzed cyclization of 1-ethynyl-2-isopropylbenzene **1**.

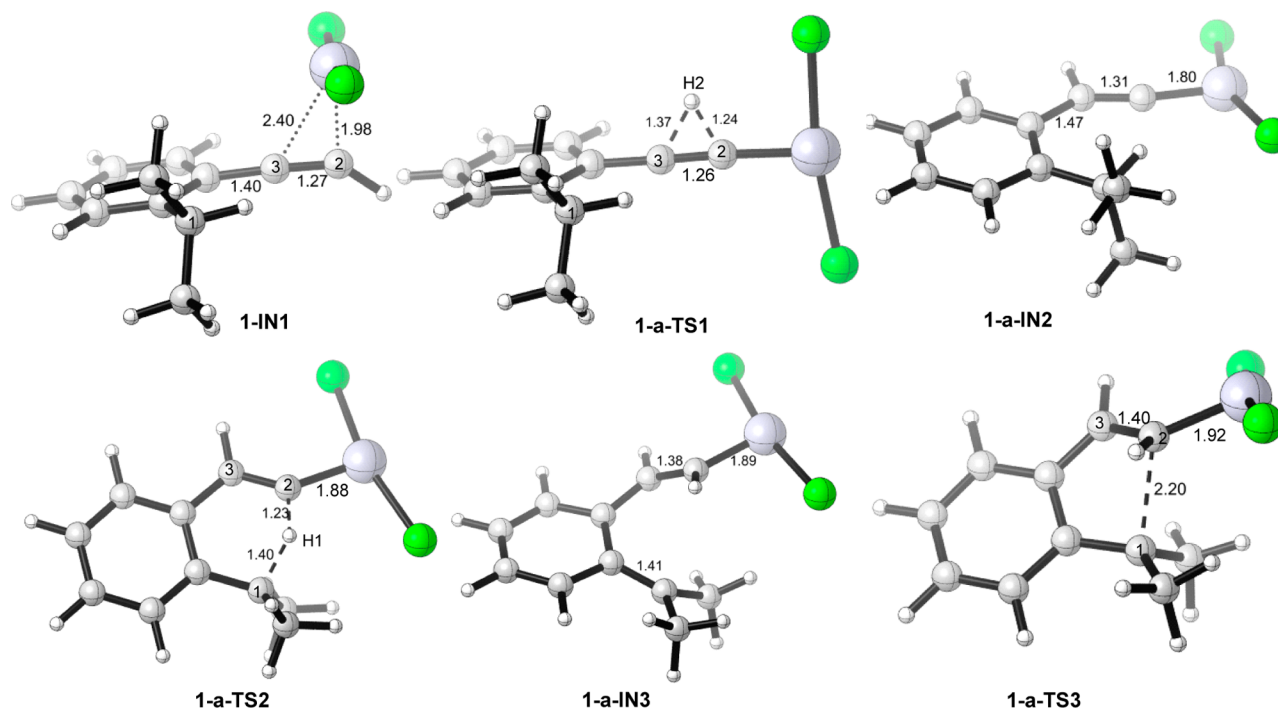


Figure 2. DFT optimized key structures for the PtCl₂-catalyzed cyclization of 1-ethynyl-2-isopropylbenzene **1** in pathway *a* (distances in Å).

energies, but M06 is better to compare the different competing pathways, see the Supporting Information for details). Solvation energies in toluene were evaluated with M06 method by a self-consistent reaction field (SCRF) using the CPCM model,²⁰ where UAKS radii²¹ were used. Solvation calculations were carried out on the gas-phase optimized structures. Unless specifically mentioned, all discussed relative energies in this paper are referred to $\Delta G_{298\text{ K}}$ (the relative gas phase free energy at 298 K). The relative enthalpies ($\Delta H_{298\text{ K}}$) in the gas phase, and the relative Gibbs free energies in toluene solution (ΔG_{sol}), both at 298 K, were also given. We must point here that geometry optimization and energy calculations in solvent using the CPCM model did not change our understanding of the investigated reactions (see discussion in the Supporting Information). All figures of structures were prepared using CYLView.²²

RESULTS AND DISCUSSION

1. Mechanism of the Cyclization of 1-Ethynyl-2-isopropylbenzene **1 (Substrate **S** with R = H, Scheme 3).** DFT calculations revealed that pathway *a* is the most favored for the cyclization of 1-ethynyl-2-isopropylbenzene **1**. In this part, we will discuss our understanding of the favored pathway *a* in detail (relative energies are given in Figure 1, while some key computed structures are given in Figure 2). The disfavored pathways *b* and *c* of this reaction will be discussed briefly later on.

Catalyst Transfer. The catalytic cycle starts from the catalyst transfer between product-catalyst complex **1-a-IN4** (which is generated in the previous catalytic cycle) and the substrate **1**. This process is endergonic by 5.0 kcal/mol, giving an alkyne–Pt complex **1-IN1**.

Complex **1-IN1** is a polarized complex with distances between the coordinated Pt and two sp-hybridized carbon atoms of 1.98 (Pt–C2) and 2.40 Å (Pt–C3), respectively (Figure 2). This unsymmetrical coordination mode implies that

1-IN1 can be regarded as a zwitterionic species with negative charge at the PtCl₂ part and the positive at the C3 atom. The cationic C3 atom can be envisioned as a vinyl cation. NBO analysis²³ shows that the charge populations on C2 and C3 in free reactant **1** are –0.21 e and –0.04 e, respectively, while these are changed to –0.27 and 0.12 e in **1-IN1**. NBO analysis also shows that Pt–C3 is a single bond, while Pt–C2 has some double-bond character, as demonstrated by the bond orders of Pt–C3 (0.99) and Pt–C2 (1.4). Thus, the Pt–C2 bond can also be described as a platinum carbene species. The favorable generation of the unsymmetrical complex **1-IN1** could be comprehended by the fact that the positive charges on C3 atom can be better stabilized by the aryl group. Thus, the triple bond in C3 position in **1-IN1** has attribute of a vinyl cation.²⁴

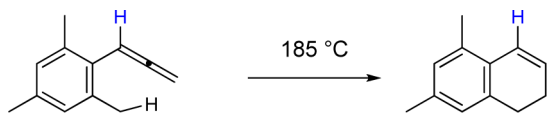
[1,2]-H Shift to Generate Vinylidene Complex. Complex **1-IN1** then undergoes a [1,2]-H shift²⁵ process to give vinylidene platinum intermediate **1-a-IN2**. This step requires an activation free energy of 18.6 kcal/mol in the gas phase and is endergonic by only 1.5 kcal/mol. IRC calculations unambiguously confirmed the connection of **1-a-TS1** to its corresponding reactant and product. In the [1,2]-H shift transition state **1-a-TS1**, the C2–Pt bond is nearly formed while the hydrogen is transferring from C2 to C3 with distances of C2–H2 and C3–H2 of 1.24 and 1.37 Å, respectively. Different groups have different barriers for the [1,2]-R migration and this difference is one reason for the different pathways (Scheme 4. The other migrations will be discussed later on).

[1,5]-H Shift. Intermediate **1-a-IN2** is then converted to the benzyl cation intermediate **1-a-IN3** via a [1,5]-H shift transition state **1-a-TS2**. In **1-a-TS2**, the bond distance of the breaking C1–H1 bond is 1.40 Å. The computed activation free energy of this step is only 5.2 kcal/mol, and the formation of **1-a-IN3** is a thermodynamically favored process, which is exergonic by 2.8 kcal/mol.

Experimentally, the [1,5]-sigmatropic hydrogen shift is widely used in organic synthesis,²⁶ but usually harsh reaction

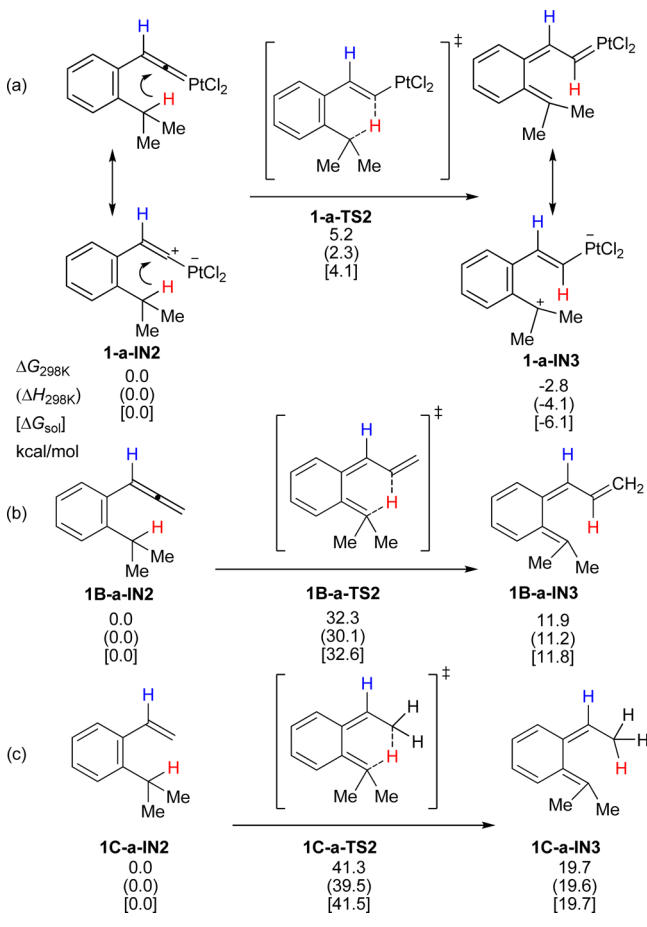
conditions are required.²⁷ For example, thermal cyclization of 2-alkyl-1-allenylbenzenes actually proceeds at 185 °C (Scheme 5).²⁸

Scheme 5. Thermal Cyclization of 2-Alkyl-1-allenylbenzene



Why is the [1,5]-H shift in the present vinylidene system so easy? To answer it, we computed the activation barriers of several [1,5]-H shift processes (Scheme 6). Calculations

Scheme 6. Different [1,5]-H Shift Processes

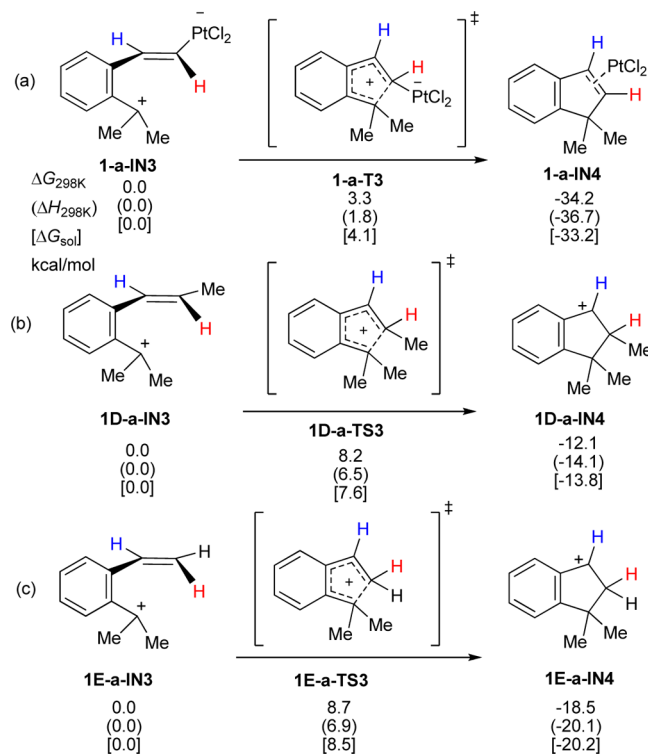


showed that the [1,5]-H shift of allenyl- and alkenyl-substituted precursors (1B-a-IN2 and 1C-a-IN2) have activation free energies of 32.3 and 41.3 kcal/mol, about 25–30 kcal/mol higher than [1,5]-H shift in the Pt–vinylidene system. We attributed the lower activation barrier for the Pt–vinylidene system to the following two reasons. One is that this Pt–vinylidene is polarized and can be regarded as a zwitterionic species with positive charge at C2 atom and negative charge at the PtCl₂ moiety. Consequently, [1,5]-hydride shift for this system is easier for the shifting hydride to the cationic C2 atom. The second reason is that the [1,5]-H shift is endothermic for 1B-a-IN2 and 1C-a-IN2, while for the Pt–vinylidene system 1-a-IN2, this is exothermic. On the basis of the Hammond Postulate,²⁹ the [1,5]-H shift reaction which is exothermic

should be easier in the Pt–vinylidene system than the other reactions shown in Scheme 6, which are endothermic.

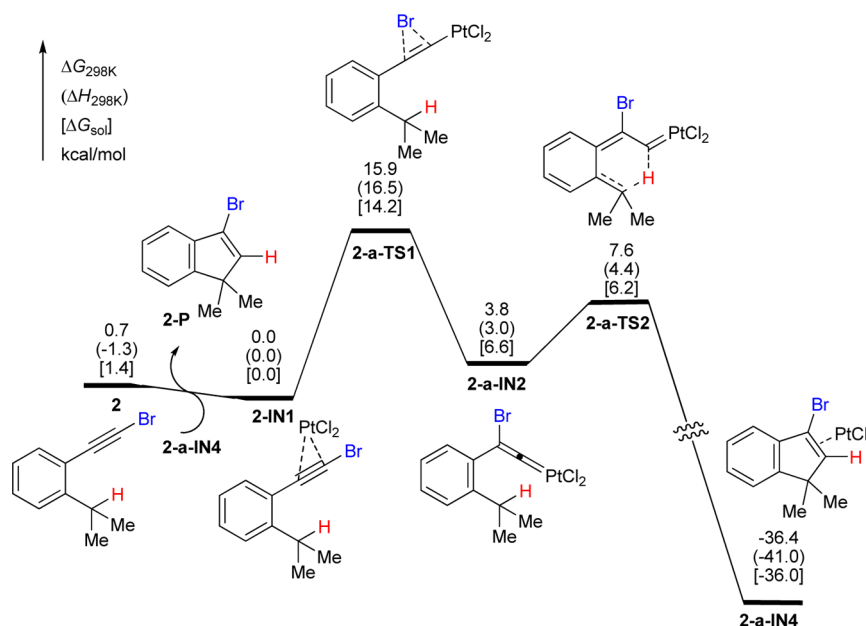
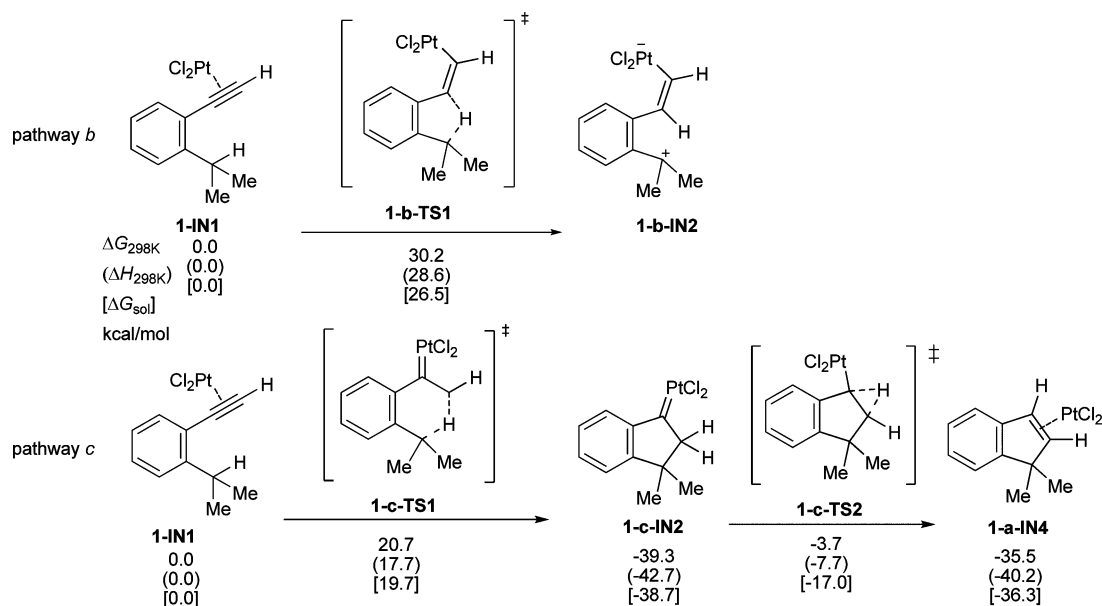
Cationic 4 π -Electrocyclization Step. Chatani proposed that intermediate **D** in pathway *a* undergoes six-electron electrocyclization to give Pt(IV) complex **E**, which then gives the final indene product via reductive elimination reaction. Similar mechanism has been proposed by Liu in the Ru-catalyzed indene and analogue synthesis.⁵ However, all efforts to locate such a 6 π -electron electrocyclization transition state failed. Instead, we can locate C1–C2 bond formation transition state 1-a-TS3. IRC calculations found such a transition state leads to indene–PtCl₂ complex 1-a-IN4, in which PtCl₂ coordinates to the alkene's double bond. This cationic 4 π -electrocyclization step is exergonic by 34.2 kcal/mol and is very facile with an activation free energy of 3.3 kcal/mol. This facile cyclization reaction can be envisioned as a 4 π -electrocyclization because 1-a-IN3 can be regarded as a vinyl-substituted benzyl cation. For comparison, we computed the simple vinyl benzyl cation's cyclization of 1D-a-IN3 and 1E-a-IN3, finding that these processes are easy with activation free energies of 8.2 and 8.7 kcal/mol, respectively (Scheme 7).

Scheme 7. Different 4 π -Electrocyclizations



In summary, the overall potential energy surface of pathway *a* shows that the first [1,2]-hydride shift is the rate-limiting step of the cyclization (Figure 1) and the activation free energy for the cyclization reaction is 23.6 kcal/mol in the gas phase. The whole catalytic cycle is highly exergonic by 30.5 kcal/mol.

Why Pathways b and c are Not Favored? Besides pathway *a*, the reaction could also occur via pathway *b*, in which a [1,4]-H shift first occurs to give 1-b-IN2. Then 1-b-IN2 gives the final product via the 4 π -electron electrocyclization reaction (Scheme 8). This mechanism has been ruled out by deuterium labeling experiments.⁶ Calculations also found that this pathway is not favored compared to pathway *a* because the energy

Scheme 8. Computed Activation Energies of Some Key Steps in Pathways *b* and *c* of Substrate 1Figure 3. DFT computed energy surface for the PtCl_2 -catalyzed cycloaddition of 1-(bromoethynyl)-2-isopropylbenzene **2** in pathway *a*.

barrier of [1,4]-hydride shift via **1-b-TS1** is as high as 30.2 kcal/mol from **1-IN1**, 11.6 kcal/mol higher than that required in pathway *a*.

The direct insertion of π -alkyne–Pt into a benzylic C–H bond via pathway *c* can also be excluded. As shown in Scheme 8, the first step for formation of cyclopentane platinum carbene intermediate **1-c-IN2** through **1-c-TS1** via an irreversible [1,5]-H shift is predicted to be more difficult than the [1,2]-H shift via **1-a-TS1**, with an activation free energy of 20.7 kcal/mol from **1-IN1** to **1-c-TS1**. This process can be viewed as the [1,5]-H shift to generate a zwitterionic species, which quickly cyclizes to give **1-c-IN2** (Scheme 8). The cyclization step can also be viewed as a 4π -electron electrocyclicization. The formation of **1-c-IN2** from **1-IN1** is dramatically exergonic by 39.3 kcal/mol as the result of the formation of a new C–C bond in this process. In addition, the computed activation free

energy of the [1,2]-H shift via **1-c-TS2** would be 35.6 kcal/mol from **1-c-IN2** to **1-a-IN4**, probably due to the very stable of platinum–carbene intermediate **1-c-IN2**. The irreversible [1,5]-H shift in the gas phase in pathway *c* is disfavored by only 2.1 kcal/mol than that of the [1,2]-H shift in pathway *a*, but this is disfavored further to 3.4 kcal/mol in toluene, suggesting that pathway *c* is completely suppressed in solution compared to pathway *a*.

From the above Results and Discussion, we can find that for 1-ethynyl-2-isopropylbenzene, the preferred pathway *a* involves the first formation of the vinylidene intermediate **1-a-IN2** via a [1,2]-H shift of the acetylenic hydrogen. This step is the rate-determining step and requires an activation free energy of 23.6 kcal/mol. Then a [1,5]-H shift of benzylic hydrogen occurs to form the vinyl benzyl cation intermediate, which could be transformed into the product–catalyst complex easily via the

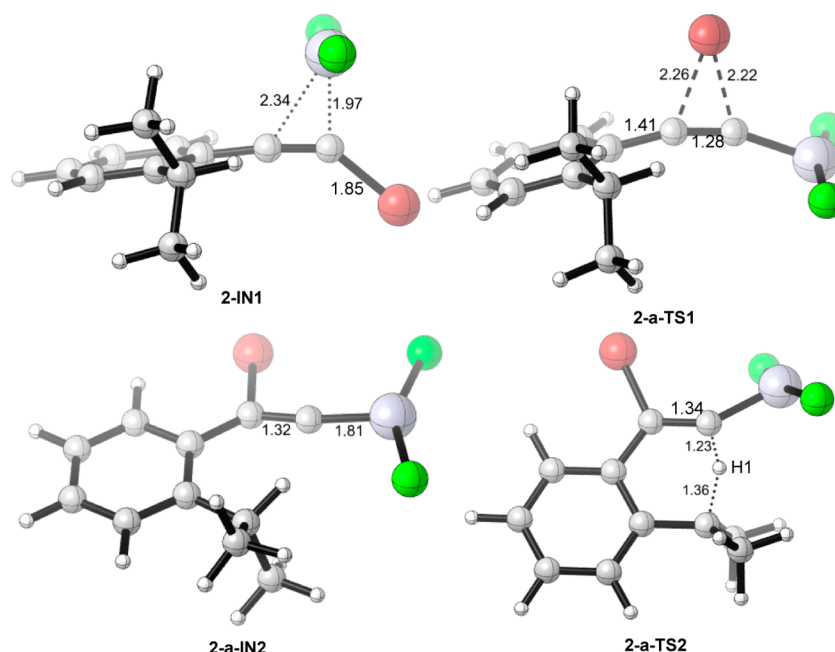


Figure 4. DFT optimized key structures for the PtCl_2 -catalyzed cyclization of 1-(bromoethynyl)-2-isopropylbenzene **2** in pathway *a* (distances in Å).

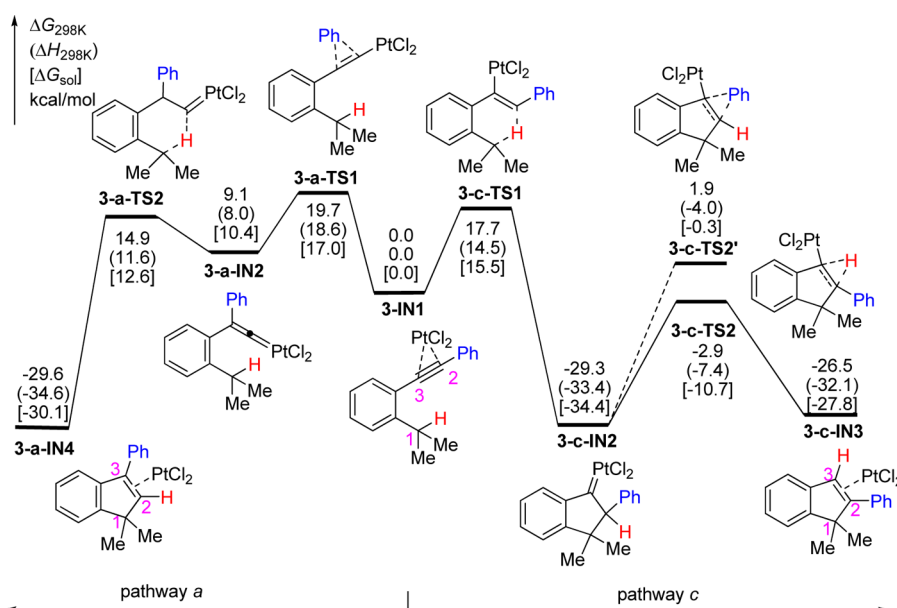


Figure 5. DFT computed energy surfaces of pathways *a* and *c* for the PtCl_2 -catalyzed cycloaddition of 1-isopropyl-2-(phenylethynyl)benzene **3-C₆H₅**.

direct 4π -electron electrocyclicization. Pathway *b* involving [1,4]-H shift and pathway *c* involving [1,5]-H shift both require higher activation free energies and are not favored compared to pathway *a*.

2. Mechanism of the Cyclization of 1-(Bromoethynyl)-2-isopropylbenzene **2 (Substrate **S** with $\text{R} = \text{Br}$, Scheme 3).** Figure 3 gives the DFT-computed energy surface of the $\text{Pt}(\text{II})$ -catalyzed intramolecular cyclization of 1-(bromoethynyl)-2-isopropylbenzene **2** in the favored pathway *a*, which also starts from catalyst transferring to the triple bond of substrate from catalyst–product complex **2-a-IN4**, followed by a [1,2]-Br shift to give vinylidene–platinum complex **2-a-IN2** with an activation free energy of 15.9 kcal/mol (for some key structures, see Figure 4). The following steps in the present

system are different from the reaction of 1-ethynyl-2-isopropylbenzene, where complex **1-a-IN2** undergoes [1,5]-H shift and 4π -electron electrocyclicization separately to give **1-a-IN4**. In the present system, **2-a-IN2** can form **2-a-IN4** in one step via a [1,5]-H shift **2-a-TS2**, requiring an activation free energy of 3.8 kcal/mol (Figure 4). This suggests that the intermediate generated by the [1,5]-H shift step is not a minimum in the reaction but it directly undergoes the 4π -electron electrocyclicization to give **2-a-IN4**.³⁰ It is interesting to note that the second step of [1,5]-H shift has a negative barrier in toluene solution, suggesting that this step is very fast.

Calculations found that the rate-determining step in pathway *a* is the [1,2]-Br shift via transition state **2-a-TS1**. The overall activation free energy for the pathway *a* is 15.9 kcal/mol. This

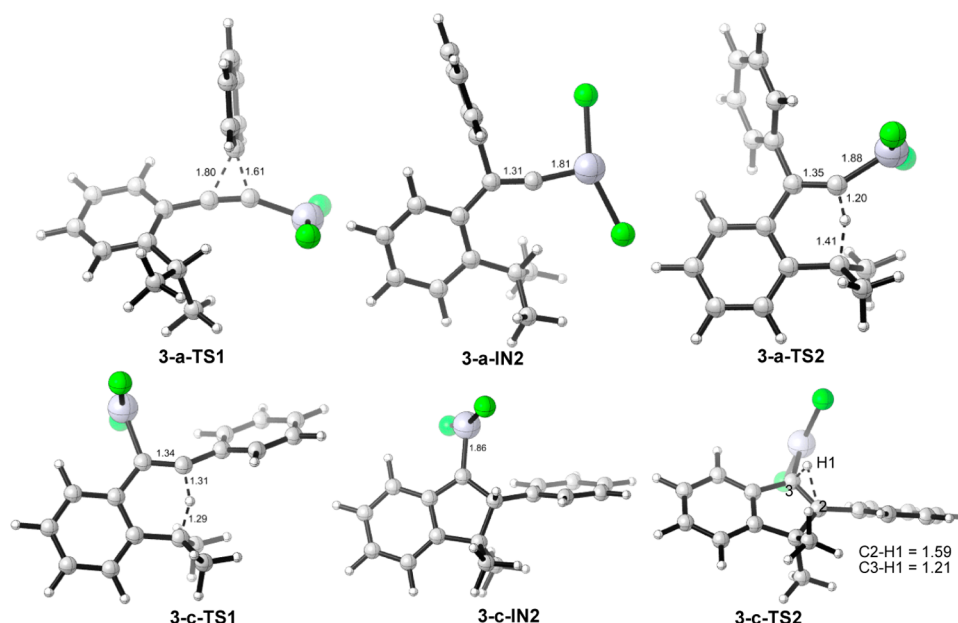


Figure 6. DFT optimized key structures for the PtCl_2 -catalyzed cycloaddition of 1-isopropyl-2-(phenylethynyl)benzene $3\text{-C}_6\text{H}_5$ in pathways *a* and *c* (distances in Å).

is similar to the reaction of **1**, which has the [1,2]-H shift step as the rate-determining step with an activation energy of 23.6 kcal/mol. This suggests that **2** is more reactive than **1** under the catalysis of PtCl_2 . Calculation results are consistent with the experimental observations (Scheme 2).⁶

We also computed the energy surfaces for pathway *b* and *c*. The [1,4]-H shift step in pathway *b* and the [1,5] hydride shift step in pathway *c* require an activation free energy of 25.0 and 20.4 kcal/mol in the gas phase, respectively. Because both pathways *b* and *c* need higher activation barriers than pathway *a* has, 1-bromoethynyl-2-isopropylbenzene prefers pathway *a* to generate indene product.

3. Mechanism of Cyclization of 1-Isopropyl-2-(phenylethynyl)benzene $3\text{-C}_6\text{H}_5$ (Substrate **S with $\text{R} = \text{Ph}$, Scheme 3).** We computed the energy surfaces of phenyl substituted compound $3\text{-C}_6\text{H}_5$ for pathways *a*, *b*, and *c* (Figures 5 and 6). The [1,4]-H shift for pathway *b* has an activation energy of 30.2 kcal/mol, which is significantly higher than those in pathways *a* and *c*, so pathway *b* can be ruled out for further consideration (Scheme 4 and Figure 5).

In pathway *a*, the first step of [1,2]-Ph migration reaction is the rate-determining step, which requires an activation free energy of 19.7 kcal/mol. The second step is a concerted [1,5]-hydride shift and cationic 4π -electrocyclization reaction, which is easy with an activation free energy of 5.8 kcal/mol (for ligand transfer reactions, see the Supporting Information).

But to our surprise, we found that pathway *c* is favored over pathway *a* by about 2.0 kcal/mol. The first step in pathway *c* is [1,5]-hydride shift and cationic 4π -electrocyclization, requiring an activation free energy of 17.7 kcal/mol. This step is exergonic by 29.3 kcal/mol. The final step in pathway *c* is the [1,2]-H shift to give indene- PtCl_2 complex **3-c-IN3** via transition state **3-c-TS2**. This step requires an activation free energy of 26.4 kcal/mol.³¹ Compared to the [1,2]-H shift for 1-ethynyl-2-isopropylbenzene **1**, which requires an activation free energy of 35.6 kcal/mol (Scheme 8), the present [1,2]-H shift is much easier. This is because the phenyl group can stabilize the transition state through conjugation. Besides, the benzylic C–H

bond is weaker than the ordinary C–H bond in the previous case.

There is a possible [1,2]-Ph shift step in pathway *c* to compete with the [1,2]-H shift from intermediate **3-c-IN2**, but this step can be ruled out due to its higher activation energy (this reaction is difficult than the [1,2]-H shift by 4.8 kcal/mol, see Figure 5). Calculations suggested that in pathway *c*, the [1,2]-H shift is the rate-determining step with the activation free energy of 26.4 kcal/mol in the gas phase.

Calculations indicated that the [1,5]-hydride shift and cyclization in pathway *c* is irreversible, and this step is easier than the rate-determining [1,2]-H shift in pathway *a* by 2.0 kcal/mol (in solution, the energy difference is reduced to 1.5 kcal/mol), suggesting that the C2-phenyl substituted product $3\text{P-C}_6\text{H}_5$ is the major product, while C3-phenyl substituted product $3\text{P}'\text{-C}_6\text{H}_5$ is the minor product (Figure 5). In He's experimental result, only $3\text{P-C}_6\text{H}_5$ was isolated and reported (Scheme 2, reaction 3).⁷ To test whether our calculation prediction was correct or not, we repeated this experiment (Scheme 9 and Table 1).

To our delight, we found that both products **3-P** and **3-P'** can be obtained with a ratio of 3.0:1 when $\text{Ar} = \text{Ph}$ (Figure 7). This suggests that the energy preference for the pathway *c* over pathway *a* is 0.9 kcal/mol. Our computed energy difference here is overestimated by 0.6 kcal/mol in the solution (1.1 kcal/mol in the gas phase). We further reasoned that this energy

Scheme 9. Cyclizations of Aryl Substituted Alkynes **3** (Reaction Yields and the Ratios of Products Are Given in Table 1)

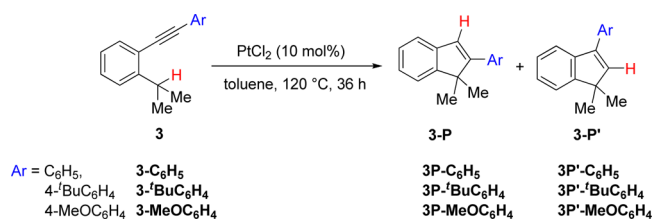
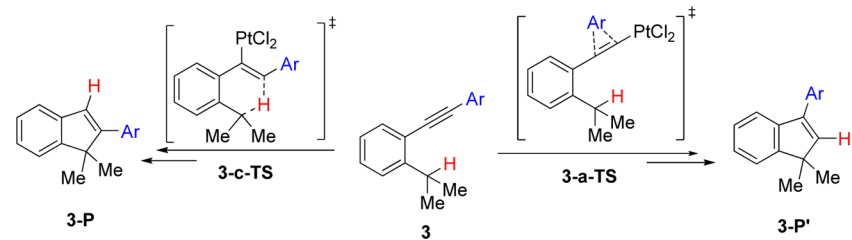


Table 1. Experimental and Computational Study of the Product Distribution for PtCl₂ Catalyzed Cyclization of **3** with Different Ar Groups



entry ^a	Ar	3-a-TS ^{b,c}	3-c-TS ^{b,c}	DFT predicted ratio in solution at 120 °C (3-P:3-P')	experimentally measured ratio (3-P:3-P')	total yield of 3-P and 3-P' (%)
1	C ₆ H ₅	17.0 (19.7)	15.5 (17.7)	6.8:1	3.0:1	43
2	4- ^t BuC ₆ H ₄	15.2 (18.4)	15.0 (17.4)	1.3:1	2.6:1	63
3	4-MeOC ₆ H ₄	16.7 (19.2)	16.0 (18.0)	2.4:1	1.9:1	70

^aThe reaction was catalyzed by 10 mol% PtCl₂ in toluene (see Scheme 9). ^bThe computed free energy in kcal/mol in toluene was relative to that of 3/PtCl₂ complex. ^cThe value in the parentheses is the computed activation free energy in the gas phase.

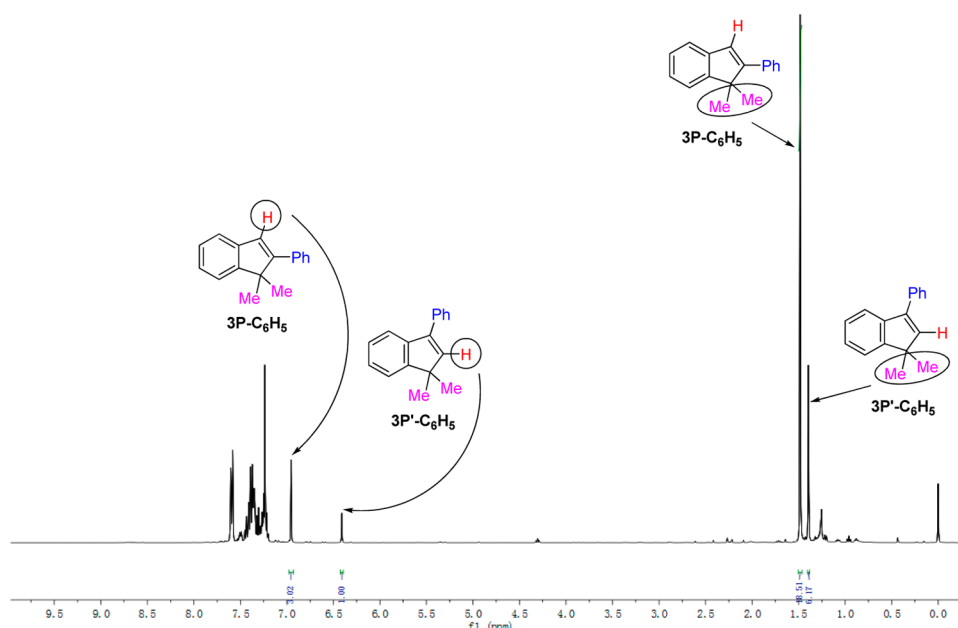


Figure 7. ¹H NMR of mixture from the cyclization reaction (36 h) of **3-C₆H₅** catalyzed by PtCl₂ at 120 °C after removing catalyst by flash chromatography on silica gel.

difference could be changed by introducing different substituents in the aryl group, and consequently, the ratio of the two products could be changed, too. Calculations indicated that the energy preference of pathway *c* over *a* was about 1 kcal/mol when a *t*-Bu or a MeO group was introduced in the aryl group, suggesting that more **3-P'** would be generated (Table 1). Our new experiments also supported the calculation results because the ratios of **3-P** to **3-P'** in these two cases were 2.6:1 and 1.9:1, respectively.

Experimentally, He and co-workers used both PtCl₂ and CuBr as the catalysts. At this moment, we do not know how the CuBr can facilitate the reaction. But we found that using He's reaction conditions, both products **3-P** and **3-P'** were obtained, in contrast to their previous reports (see the Experimental Section). This suggested that pathways *a* and *c* could both take place when both catalyst of PtCl₂ and additive of CuBr were used. Further investigation on how CuBr affects the reaction will be carried out.

4. Mechanism of the Cyclization of 1-Isopropyl-2-(prop-1-ynyl)benzene 4-CH₃ (Substrate **S with R = Me, Scheme 3).** Experimentally, He and co-workers carried out the indene synthesis using R = alkyl group in their optimized reaction conditions (PtCl₂, CuBr) but not under the PtCl₂ catalysis conditions. We were interested to know what could happen for this system using PtCl₂ as the only catalyst. Our DFT calculations found that for reaction 4, the pathway *c* is the most favored (Figures 8, 9 and Scheme 4). The [1,5]-H shift/cyclization via **4-c-TS1** and [1,2]-H shift step via **4-c-TS2** require activation free energies of 21.5 and 25.4 kcal/mol, respectively. The corresponding [1,2]-Me shift for pathway *a* requires an activation free energy of 31.6 kcal/mol, indicating that C3 substituted product is difficult to be generated. We carried out an experiment to test this, showing that our calculations agreed with the new experiment. The cycloisomerization of **4-CH₂CH₂Ph** (substrate **4** with R = CH₂CH₂Ph) gave a single C2 substituted product (see Scheme 2 and Experimental Section).

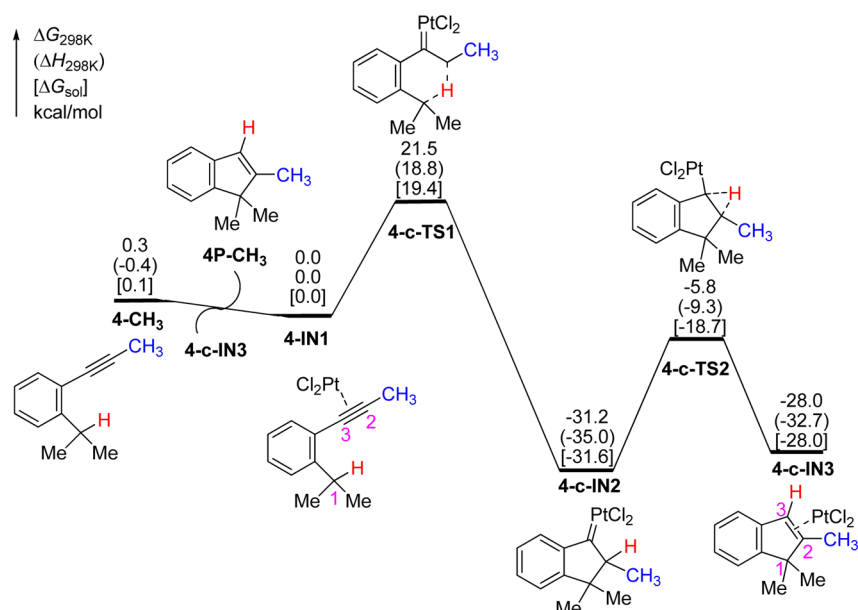


Figure 8. DFT computed energy surface of pathway *c* for the PtCl₂-catalyzed cycloaddition of 1-isopropyl-2-(prop-1-ynyl)benzene **4-CH₃**.

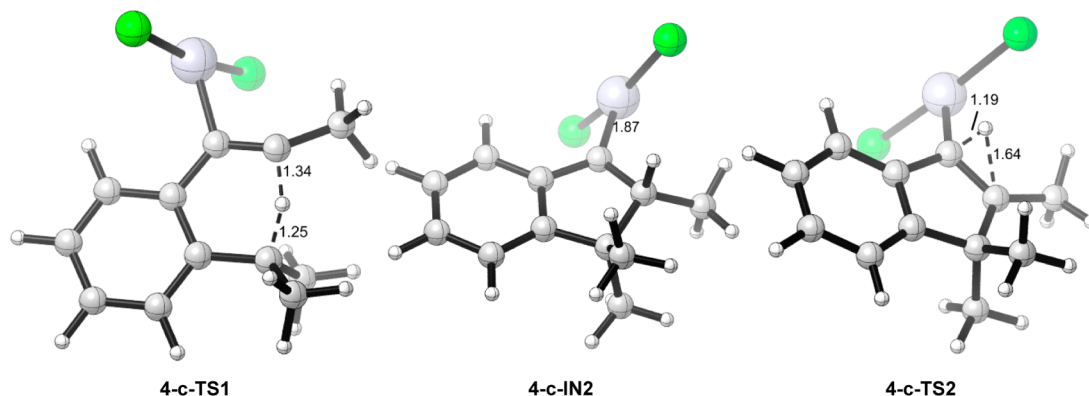
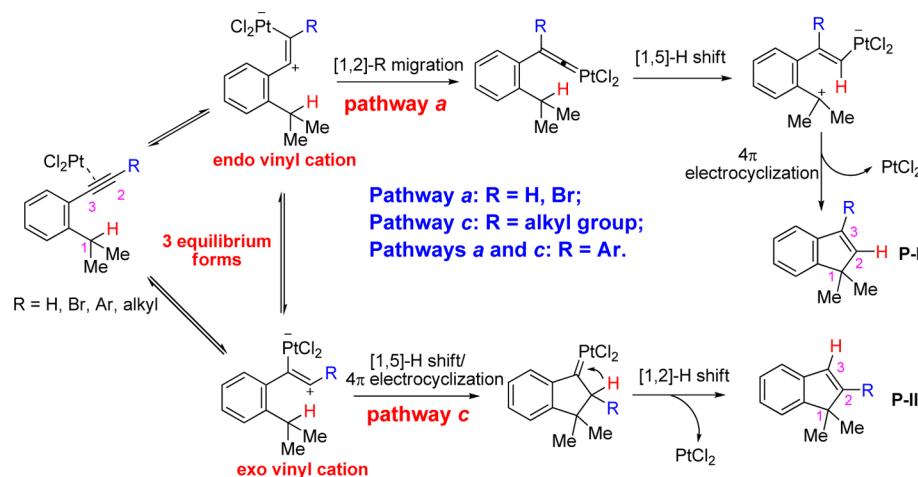


Figure 9. DFT optimized key structures for the PtCl₂-catalyzed cycloaddition of 1-isopropyl-2-(prop-1-ynyl)benzene **4-CH₃** (distances in Å).

Scheme 10. Competing Pathways of PtCl₂-Catalyzed Cyclization of *o*-Isopropyl Substituted Aryl Alkynes and How Substituents Affect the Regiochemistry



5. Competition of [1,2]-R Migration and [1,5]-H shift is Key to Determine the Reaction Pathway. Through DFT calculations, three modes of sp³ C–H activation shown in Schemes 3 and 4 have been investigated. We found the most

efficient C–H activation is from intermediate C (vinylidene complex) to D in pathway *a* with activation free energy of about 5 kcal/mol. The C–H activation via [1,5]-H shift from H to I in pathway *c* usually requires activation free energies of

about 17–20 kcal/mol. The most difficult C–H activation is through [1,4]-H shift from endo vinyl cation in pathway *b*, with activation free energies of about 25–30 kcal/mol. Due to these reasons, pathway *b* is not operative for the C–H activation. Because C–H activations in pathways *a* and *c* are easy, the competition between pathways *a* and *c* is determined by the [1,2]-R migration step and [1,5]-H shift. The results shows that easier [1,2]-migration (when R = H and Br) favors pathway *a* while difficult migration (when R = alkyl group) prefers pathway *c*. When R = aryl group, pathways *a* and *c* have very close activation energies due to the competitive [1,2]-Ar migration and [1,5]-H shift, and consequently two products can be obtained (Scheme 10). This prediction was supported by new experiments.

CONCLUSIONS

We scrutinized computationally and (in some cases) experimentally the mechanisms of platinum(II)-catalyzed intramolecular cyclization of *ortho*-substituted aryl alkynes involving a key step of sp³ C–H bond activation. We evaluated the feasibility of three pathways proposed by Chatani, He, and us for four different substrates with the different R substituents (R = H, Br, Ph, and Me) in the alkyne part. Calculations found that for substrates with R = H or Br, these reactions favor pathway *a* to undergo [1,2]-H and [1,2]-Br migrations from the endo vinyl cations, generating Pt–vinylidene complexes. Then facile [1,5]-H shifts and 4π-electrocyclization (in two-step or one-step) furnish the indene products. H and Br atoms in this pathway migrate from the original terminal position of the alkyne to the C3 position of the indenenes. For substrate with R = Me, the reaction reacts through pathway *c*, starting from irreversible [1,5]-H shift from exo vinyl cation species. The competing pathway *a* via [1,2]-methyl migration is very difficult and cannot take place. Consequently, the alkyl group is still at the C2 position of the indene products. For substrates with R = Ar, DFT calculations indicated that both pathways *a* and *c* can take place, leading to two indene products. Major product with Ph at C2 position was obtained through pathway *c*, and the minor product with Ph at C3 position was obtained through pathway *a*. The prediction was further supported by the new experiments. The in-depth understanding of the present three C–H activation modes will be helpful for the future design of new C–H activation reactions.

EXPERIMENTAL SECTION

General Information. Toluene was dried over Na before use. Reaction temperatures refer to the external temperature or to the temperature of the bath in which the reaction vessel was partially immersed. Data for ¹H NMR (400 MHz) spectra are reported as follows: chemical shift (ppm, referenced to TMS; s = singlet, d = doublet, t = triplet, q = quartet, dd = doublet of doublets, dt = doublet of triplets, ddd = doublet of doublet of doublets, ddt = doublet of doublet of triplets, m = multiplet), coupling constant (Hz), and integration. Data for ¹³C NMR (100 MHz) are reported in terms of chemical shift (ppm) relative to residual solvent peak (CDCl₃: 77.0 ppm). Infrared spectra are reported in wavenumbers (cm⁻¹). HRMS were performed under ESI ionization technique using FT-ICR analyzer. PE = petroleum ether, EA = ethyl acetate.

1-((4-*tert*-Butylphenyl)ethynyl)-2-isopropylbenzene (**3-^tBuC₆H₄**). To a stirred mixture of 1-iodo-2-isopropylbenzene (493.4 mg, 2.00 mmol), PdCl₂(PPh₃)₂ (70.2 mg, 0.10 mmol), and CuI (38.1 mg, 0.20 mmol) in NEt₃ (3 mL), 4-*tert*-butylphenylacetylene (348.1 mg, 2.20 mmol) was added dropwise at 0 °C. The mixture was then stirred at room temperature overnight. On completion, the mixture was passed

through a pad of Celite. The filtrate was concentrated in a vacuum, and the residue was purified by flash chromatography on silica gel (eluted with PE) to afford the product as a white solid (532.3 mg, 95%). R_f = 0.45 (PE), mp: 50–52 °C. ¹H NMR (400 MHz, CDCl₃): δ 7.60–7.55 (m, 3H), 7.47–7.44 (m, 2H), 7.38–7.34 (m, 2H), 7.26–7.21 (m, 1H), 3.71–3.60 (m, 1H), 1.41–1.39 (m, 15H). ¹³C NMR (100 MHz, CDCl₃): δ 151.5, 150.5, 132.3, 131.3, 128.6, 125.6, 125.4, 125.0, 122.3, 120.7, 93.3, 87.7, 34.8, 31.8, 31.3, 23.2. IR (neat): 2969, 1516, 1482, 1468, 1367, 1270 cm⁻¹. HRMS (ESI): calcd for C₂₁H₂₅ (M + H)⁺, 277.1951; found, 277.1958.

General Cyclization Procedure Using PtCl₂ as Catalyst (Schemes 2 and 9). PtCl₂ (10 mol% to the substrate) was charged in a base-washed, oven-dried Schlenk flask under an atmosphere of nitrogen, and then a solution of the alkyne substrate in dried toluene was added. The reaction mixture was stirred at 120 °C for 36 h. After being cooled to room temperature, the mixture was concentrated and the residue was purified by flash column chromatography with silica gel to afford the mixture of cycloadducts.

1-Isopropyl-2-(phenylethynyl)benzene (**3-C₆H₅**)⁷ (23.0 mg, 0.10 mmol), PtCl₂ (3.0 mg, 0.011 mmol), toluene (1.5 mL), eluent: PE, total yield of cycloadducts (10.0 mg, 43%), ratio of **3P-C₆H₅**⁷/**3P'-C₆H₅**³² = 3.0:1 (determined by ¹H NMR).³³

1-((4-*tert*-Butylphenyl)ethynyl)-2-isopropylbenzene (**3-^tBuC₆H₄**) (29.3 mg, 0.12 mmol), PtCl₂ (3.7 mg, 0.014 mmol), toluene (1.5 mL), eluent: PE, total yield of cycloadducts (18.4 mg, 63%), ratio of **3P-^tBuC₆H₄**/**3P'-^tBuC₆H₄** = 2.6:1 (determined by ¹H NMR).

1-Isopropyl-2-((4-methoxyphenyl)ethynyl)benzene (**3-MeOC₆H₄**)³⁴ (31.4 mg, 0.13 mmol), PtCl₂ (3.5 mg, 0.013 mmol), toluene (1.3 mL), eluent: PE to PE/EA = 100:1, total yield of cycloadducts (22.0 mg, 70%), ratio of **3P-MeOC₆H₄**⁷/**3P'-MeOC₆H₄** = 1.9:1 (determined by ¹H NMR).

1-Isopropyl-2-(4-phenylbut-1-ynyl)benzene (**4-CH₂CH₂Ph**)⁷ (40.6 mg, 0.16 mmol), PtCl₂ (4.3 mg, 0.016 mmol), toluene (3.0 mL), eluent: PE, conversion 71%, yield of **4P-CH₂CH₂Ph**⁷ (6.4 mg, brsm 22%). This reaction is not clean because we obtained a mixture of substrate and product and the yield of product was determined by ¹H NMR from the isolated mixture of substrate and product. In He's experiment using both PtCl₂ and CuBr, the reaction yield was 71%.⁷

General Cyclization Procedure using PtCl₂ as Catalyst with Additive CuBr (He's Original Procedure).⁷ PtCl₂ (10 mol% to the substrate) and CuBr (2 equiv to the substrate) were charged in a base-washed, oven-dried Schlenk flask under an atmosphere of nitrogen. Then a solution of the alkyne substrates in dried toluene was added. The solution was then stirred at 120 °C for 36 h. After being cooled to room temperature, the mixture was concentrated and the residue was purified by flash column chromatography with silica gel to give the cycloaddition products.

1-Isopropyl-2-(phenylethynyl)benzene (**3-C₆H₅**)⁷ (23.0 mg, 0.10 mmol), PtCl₂ (3.0 mg, 0.011 mmol), CuBr (28 mg, 0.20 mmol), toluene (1.5 mL), eluent: PE, total yield of cycloadducts (17.7 mg, 77%), ratio of **3P-C₆H₅**⁷/**3P'-C₆H₅**³² = 3.0:1 (determined by ¹H NMR).

1-((4-*tert*-Butylphenyl)ethynyl)-2-isopropylbenzene (**3-^tBuC₆H₄**) (31.8 mg, 0.12 mmol), PtCl₂ (3.7 mg, 0.014 mmol), CuBr (40.2 mg, 0.28 mmol), toluene (1.5 mL), eluent: PE, total yield of cycloadducts (27.4 mg, 86%), ratio of **3P-^tBuC₆H₄**/**3P'-^tBuC₆H₄** = 2.5:1 (determined by ¹H NMR).

1-Isopropyl-2-((4-methoxyphenyl)ethynyl)benzene (**3-MeOC₆H₄**)³⁴ (29.2 mg, 0.12 mmol), PtCl₂ (3.2 mg, 0.012 mmol), CuBr (34.4 mg, 0.24 mmol), toluene (1.3 mL), eluent: PE to PE/EA = 100:1, total yield of cycloadducts (25.7 mg, 88%), ratio of **3P-MeOC₆H₄**/**3P'-MeOC₆H₄** = 1.8:1 (determined by ¹H NMR).

Test of Whether Additive of D₂O or CD₃OD Could Catalyze the [1,2]-H Shift in the PtCl₂ Catalyzed Cyclization. Similar to the general cyclization procedure using PtCl₂ as catalyst except for 5 equiv of D₂O or CD₃OD was added to the Schlenk flask before heating. For D₂O: 1-isopropyl-2-((4-methoxyphenyl)ethynyl)benzene (**3-MeOC₆H₄**) (27.8 mg, 0.10 mmol), PtCl₂ (2.7 mg, 0.010 mmol), toluene (1.0 mL), D₂O (10.0 mg, 0.50 mmol), eluent: PE to PE/EA = 100:1, conversion 65%, total yield of cycloadducts (15.5 mg, brsm 86%), ratio of **3P-MeOC₆H₄**/**3P'-MeOC₆H₄** = 1.9:1 (determined by

¹H NMR). For CD₃OD: 1-isopropyl-2-((4-methoxyphenyl)ethynyl)-benzene (**3-MeOC₆H₄**), (27.4 mg, 0.099 mmol), PtCl₂ (2.6 mg, 0.0099 mmol), toluene (1.0 mL), CD₃OD (18.0 mg, 0.50 mmol), eluent: PE to PE/EA = 100:1, total yield of cycloadducts (22.6 mg, 82%), ratio of **3P-MeOC₆H₄**/**3P'-MeOC₆H₄** = 1.7:1 (determined by ¹H NMR).

1,1-Dimethyl-2-phenyl-1H-indene (3P-C₆H₅).⁷ Colorless oil; R_f = 0.35 (PE). ¹H NMR (400 MHz, CDCl₃): δ 7.65–7.63 (m, 2H), 7.45–7.39 (m, 4H), 7.36–7.31 (m, 1H), 7.30–7.24 (m, 2H), 7.00 (s, 1H), 1.53 (s, 6H). ¹³C NMR (100 MHz, CDCl₃): δ 155.9, 155.0, 141.5, 136.2, 128.4, 127.3, 127.2, 126.6, 126.0, 125.2, 121.2, 121.1, 50.8, 25.0. IR (neat): 2969, 2928, 2864, 1494, 1471, 1445, 1352, 1028 cm⁻¹. HRMS (ESI): calcd for C₁₇H₁₇ (M + H)⁺, 221.1325; found, 221.1319.

1,1-Dimethyl-3-phenyl-1H-indene (3P'-C₆H₅).³² Colorless oil; R_f = 0.41 (PE). ¹H NMR (400 MHz, CDCl₃): δ 7.62–7.60 (m, 2H), 7.53–7.51 (m, 1H), 7.48–7.43 (m, 2H), 7.42–7.35 (m, 2H), 7.30–7.27 (m, 2H), 6.43 (s, 1H), 1.41 (s, 6H). ¹³C NMR (100 MHz, CDCl₃): δ 154.3, 143.9, 141.7, 140.7, 135.8, 128.4, 127.6, 127.4, 126.3, 125.3, 121.4, 120.5, 48.3, 24.6. IR (neat): 2965, 2864, 2842, 1620, 1512, 1468, 1352, 1251, 1177, 1039 cm⁻¹. HRMS (ESI): calcd for C₁₇H₁₇ (M + H)⁺, 221.1325; found, 221.1323.

2-(4-tert-Butylphenyl)-1,1-dimethyl-1H-indene (3P-tBuC₆H₄). Light-yellow oil; R_f = 0.32 (PE). ¹H NMR (400 MHz, CDCl₃): δ 7.58–7.56 (m, 2H), 7.43–7.41 (m, 2H), 7.36–7.34 (m, 2H), 7.26–7.18 (m, 2H), 6.98 (s, 1H), 1.50 (s, 6H), 1.35 (s, 9H). ¹³C NMR (100 MHz, CDCl₃): δ 155.6, 155.2, 150.2, 141.6, 133.0, 126.7, 126.6, 125.30, 125.29, 125.0, 121.1, 120.9, 50.7, 34.5, 31.3, 25.2. IR (neat): 2972, 2872, 1516, 1471, 1367, 1274, 1117, 1024 cm⁻¹. HRMS (ESI): calcd for C₂₁H₂₅ (M + H)⁺, 277.1951; found, 277.1953.

3-(4-tert-Butylphenyl)-1,1-dimethyl-1H-indene (3P'-tBuC₆H₄). Light-yellow oil; R_f = 0.40 (PE). ¹H NMR (400 MHz, CDCl₃): δ 7.55–7.52 (m, 3H), 7.47–7.45 (m, 2H), 7.39–7.37 (m, 1H), 7.29–7.22 (m, 2H), 6.39 (s, 1H), 1.39 (s, 6H), 1.37 (s, 9H). ¹³C NMR (100 MHz, CDCl₃): δ 154.5, 150.5, 143.7, 141.9, 140.6, 133.0, 127.3, 126.3, 125.5, 125.3, 121.5, 120.7, 48.3, 34.6, 31.4, 24.8. IR (neat): 2969, 2864, 1516, 1471, 1412, 1367, 1270, 1117, 1024 cm⁻¹. HRMS (ESI): calcd for C₂₁H₂₅ (M + H)⁺, 277.1951; found, 277.1953.

2-(4-Methoxyphenyl)-1,1-dimethyl-1H-indene (3P-MeOC₆H₄).⁷ Light-yellow oil; R_f = 0.45 (PE/EA = 50:1). ¹H NMR (400 MHz, CDCl₃): δ 7.58–7.54 (m, 2H), 7.35–7.33 (m, 2H), 7.26–7.18 (m, 2H), 6.96–6.92 (m, 2H), 6.89 (s, 1H), 3.84 (s, 3H), 1.48 (s, 6H). ¹³C NMR (100 MHz, CDCl₃): δ 158.9, 155.5, 154.9, 141.7, 128.7, 128.3, 126.6, 124.9, 124.6, 121.1, 120.8, 113.8, 55.3, 50.7, 25.1. IR (neat): 2959, 2918, 2849, 1633, 1508, 1469, 1249, 1178, 1034 cm⁻¹. HRMS (ESI): calcd for C₁₈H₁₉O (M + H)⁺, 251.1430; found, 251.1431.

3-(4-Methoxyphenyl)-1,1-dimethyl-1H-indene (3P'-MeOC₆H₄). Light-yellow oil; R_f = 0.49 (PE/EA = 50:1). ¹H NMR (400 MHz, CDCl₃): δ 7.54–7.51 (m, 2H), 7.49–7.47 (m, 1H), 7.38–7.36 (m, 1H), 7.26–7.23 (m, 2H), 6.98–6.95 (m, 2H), 6.33 (s, 1H), 3.85 (s, 3H), 1.37 (s, 6H). ¹³C NMR (100 MHz, CDCl₃): δ 159.1, 154.4, 142.9, 142.0, 140.2, 128.7, 128.4, 126.3, 125.2, 121.4, 120.5, 113.9, 55.3, 48.2, 24.7. IR (neat): 2959, 2926, 1600, 1509, 1464, 1248, 1177, 1035 cm⁻¹. HRMS (ESI): calcd for C₁₈H₁₉O (M + H)⁺, 251.1430; found, 251.1429.

■ ASSOCIATED CONTENT

☉ Supporting Information

NMR spectra of new compounds, full citation of Gaussian 09, some disfavored pathways, computed energy surface using B3LYP method, optimized Cartesian coordinates and energies. This material is available free of charge via the Internet at <http://pubs.acs.org>.

■ AUTHOR INFORMATION

Corresponding Author

*E-mail: yuzx@pku.edu.cn.

Author Contributions

[§]These authors contributed equally.

Notes

The authors declare no competing financial interest.

■ ACKNOWLEDGMENTS

We are indebted to the generous financial support from the Natural Science Foundation of China (21232001) and the National Basic Research Program of China-973 Program (2011CB808600). We thank Mr. Pei-Jun Cai and Dr. Wenbo Xu for repeating some experiments.

■ REFERENCES

- (1) (a) Lyons, T. W.; Sanford, M. S. *Chem. Rev.* **2010**, *110*, 1147. (b) Satoh, T.; Miura, M. *Chem.—Eur. J.* **2010**, *16*, 11212. (c) Chen, X.; Engle, K. M.; Wang, D.-H.; Yu, J.-Q. *Angew. Chem., Int. Ed.* **2009**, *48*, 5094. (d) Park, Y. J.; Park, J.-W.; Jun, C.-H. *Acc. Chem. Res.* **2008**, *41*, 222. (e) Lewis, J. C.; Bergman, R. G.; Ellman, J. A. *Acc. Chem. Res.* **2008**, *41*, 1013. (f) Díaz-Requejo, M. M.; Pérez, P. J. *Chem. Rev.* **2008**, *108*, 3379. (g) Davies, H. M. L.; Manning, J. R. *Nature* **2008**, *451*, 417. (h) Herrerías, C. I.; Yao, X.; Li, Z.; Li, C.-J. *Chem. Rev.* **2007**, *107*, 2546. (i) Godula, K.; Sames, D. *Science* **2006**, *312*, 67.
- (2) (a) Tauchert, M. E.; Incarvito, C. D.; Rheingold, A. L.; Bergman, R. G.; Ellman, J. A. *J. Am. Chem. Soc.* **2012**, *134*, 1482. (b) Ackermann, L. *Chem. Rev.* **2011**, *111*, 1315. (c) Sawyer, K. R.; Cahoon, J. F.; Shanoski, J. E.; Glascoe, E. A.; Kling, M. F.; Schlegel, J. P.; Zuerb, M. C.; Hapke, M.; Hartwig, J. F.; Webster, C. E.; Harris, C. B. *J. Am. Chem. Soc.* **2010**, *132*, 1848. (d) Potavathri, S.; Pereira, K. C.; Gorelsky, S. I.; Pike, A.; LeBris, A. P.; DeBoef, B. *J. Am. Chem. Soc.* **2010**, *132*, 14676.
- (3) Nakamura, I.; Bajracharya, G. B.; Wu, H.; Oishi, K.; Mizushima, Y.; Gridnev, I. D.; Yamamoto, Y. *J. Am. Chem. Soc.* **2004**, *126*, 15423.
- (4) Bajracharya, G. B.; Pahadi, N. K.; Gridnev, I. D.; Yamamoto, Y. *J. Org. Chem.* **2006**, *71*, 6204.
- (5) (a) Odedra, A.; Datta, S.; Liu, R.-S. *J. Org. Chem.* **2007**, *72*, 3289. (b) Datta, S.; Odedra, A.; Liu, R.-S. *J. Am. Chem. Soc.* **2005**, *127*, 11606.
- (6) Tobisu, M.; Nakai, H.; Chatani, N. *J. Org. Chem.* **2009**, *74*, 5471.
- (7) Yang, S.; Li, Z.; Jian, X.; He, C. *Angew. Chem., Int. Ed.* **2009**, *48*, 3999.
- (8) For selected recent transition-metal-catalyzed benzylic sp³ C-H activation reactions, see: (a) Minami, Y.; Yamada, K.; Hiyama, T. *Angew. Chem., Int. Ed.* **2013**, *52*, 10611. (b) Bhunia, S.; Ghorpade, S.; Huple, D. B.; Liu, R.-S. *Angew. Chem., Int. Ed.* **2012**, *51*, 2939. (c) Xia, J.-D.; Deng, G.-B.; Zhou, M.-B.; Liu, W.; Xie, P.; Li, J.-H. *Synlett* **2012**, *23*, 2707. (d) Zhao, S.-C.; Shu, X.-Z.; Ji, K.-G.; Zhou, A.-X.; He, T.; Liu, X.-Y.; Liang, Y.-M. *J. Org. Chem.* **2011**, *76*, 1941. (e) Zeng, X.; Ilies, L.; Nakamura, E. *J. Am. Chem. Soc.* **2011**, *133*, 17638. (f) Shu, X.-Z.; Ji, K.-G.; Zhao, S.-C.; Zheng, Z.-J.; Chen, J.; Lu, L.; Liu, X.-Y.; Liang, Y.-M. *Chem.—Eur. J.* **2008**, *14*, 10556.
- (9) Zhao and coworkers reported the mechanism of cyclization of 1-ethynyl-2-isopropylbenzene, but Br, aryl, methyl substituted compounds were not discussed, and pathway *c* proposed by us was not considered, either. See Li, Z.-F.; Fan, Y.; DeYonker, N. J.; Zhang, X.; Su, C.-Y.; Xu, H.; Xu, X.; Zhao, C. *J. Org. Chem.* **2012**, *77*, 6076.
- (10) (a) Davies, H. M. L.; Dick, A. R. *Top. Curr. Chem.* **2010**, *292*, 303. (b) Davies, H. M. L.; Beckwith, R. E. *J. Chem. Rev.* **2003**, *103*, 2861. (c) Davies, H. M. L.; Antoulinakis, E. G. *Org. Lett.* **2000**, *2*, 4153.
- (11) (a) Lynam, J. M. *Chem.—Eur. J.* **2010**, *16*, 8238. (b) Fiukamizu, K.; Miyake, Y.; Nishibayashi, Y. *Angew. Chem., Int. Ed.* **2009**, *48*, 2534. (c) Trost, B. M.; McClory, A. *Chem.—Asian J.* **2008**, *3*, 164. (d) Liu, R.-S. *Synlett* **2008**, 801. (e) Bruneau, C.; Dixneuf, P. H. *Angew. Chem., Int. Ed.* **2006**, *45*, 2176. (f) Caskey, S. R.; Stewart, M. H.; Johnson, M. J. A.; Kampf, J. W. *Angew. Chem., Int. Ed.* **2006**, *45*, 7422. (g) Nevado, C.; Echavarren, A. M. *Synthesis* **2005**, 167.
- (12) Frisch, M. J.; et al. *Gaussian 09*, revision A.02; Gaussian, Inc.: Wallingford, CT, 2010.
- (13) Parr, R. G.; Yang, W. *Density-Functional Theory of Atoms and Molecules*; Oxford University Press: Oxford, U.K., 1989.

(14) (a) Becke, A. D. *J. Chem. Phys.* **1993**, *98*, 5648. (b) Lee, C.; Yang, W.; Parr, R. G. *Phys. Rev. B* **1988**, *37*, 785.

(15) Hehre, W. J.; Radom, L.; Schleyer, P. v. R.; Pople, J. A. *Ab Initio Molecular Orbital Theory*; Wiley: New York, 1986.

(16) (a) Hay, P. J.; Wadt, W. R. *J. Chem. Phys.* **1985**, *82*, 299. (b) Dunning, T. H., Jr.; Hay, P. J. In *Modern Theoretical Chemistry*; Schaefer, H. F., III, Ed.; Plenum Press: New York, 1977; pp 1–28.

(17) (a) Huang, G.; Cheng, B.; Xu, L.; Li, Y.; Xia, Y. *Chem.—Eur. J.* **2012**, *18*, 5401. (b) Jin, L.; Wu, Y.; Zhao, X. *Organometallics* **2012**, *31*, 3065. (c) Xia, Y.; Huang, G. *J. Org. Chem.* **2010**, *75*, 7842. (d) Soriano, E.; Marco-Contelles, J. *J. Org. Chem.* **2007**, *72*, 1443. (e) Martin-Matute, B.; Nevado, C.; Cardenas, D. J.; Echavarren, A. M. *J. Am. Chem. Soc.* **2003**, *125*, 5757. (f) Mendez, M.; Munoz, M. P.; Nevado, C.; Cardenas, D. J.; Echavarren, A. M. *J. Am. Chem. Soc.* **2001**, *123*, 10511.

(18) (a) Gonzalez, C.; Schlegel, H. B. *J. Phys. Chem.* **1990**, *94*, 5523. (b) Gonzalez, C.; Schlegel, H. B. *J. Chem. Phys.* **1989**, *90*, 2154.

(19) (a) Zhao, Y.; Truhlar, D. G. *Acc. Chem. Res.* **2008**, *41*, 157. (b) Zhao, Y.; Truhlar, D. G. *Theor. Chem. Acc.* **2008**, *120*, 215.

(20) (a) Takano, Y.; Houk, K. N. *J. Chem. Theory Comput.* **2005**, *1*, 70. (b) Cossi, M.; Rega, N.; Scalmani, G.; Barone, V. *J. Comput. Chem.* **2003**, *24*, 669. (c) Barone, V.; Cossi, M. *J. Phys. Chem. A* **1998**, *102*, 1995.

(21) Barone, V.; Cossi, M.; Tomasi, J. *J. Chem. Phys.* **1997**, *107*, 3210.

(22) Legault, C. Y. *CYLview*, 1.0b; Université de Sherbrooke: Sherbrooke, Québec, Canada, 2009; <http://www.cylview.org>.

(23) Reed, A. E.; Curtiss, L. A.; Weinhold, F. *Chem. Rev.* **1988**, *88*, 899.

(24) We can locate another complex **1-IN1'** in a symmetric fashion, but it is higher in energy by 3.5 kcal/mol than **1-IN1**, see the Supporting Information.

(25) (a) Bruce, M. I. *Chem. Rev.* **1991**, *91*, 197. (b) Bruce, M. I.; Swincer, A. G. In *Advances in Organometallic Chemistry*; Stone, F. G. A., Robert, W., Eds.; Academic Press: 1983; Vol. 22, p 59.

(26) (a) Chen, L.; Zhang, L.; Lv, J.; Cheng, J.-P.; Luo, S. *Chem.—Eur. J.* **2012**, *18*, 8891. (b) Vadola, P. A.; Carrera, I.; Sames, D. *J. Org. Chem.* **2012**, *77*, 6689. (c) Sugiishi, T.; Nakamura, H. *J. Am. Chem. Soc.* **2012**, *134*, 2504. (d) Han, Y.-Y.; Han, W.-Y.; Hou, X.; Zhang, X.-M.; Yuan, W.-C. *Org. Lett.* **2012**, *14*, 4054. (e) Cao, W.; Liu, X.; Wang, W.; Lin, L.; Feng, X. *Org. Lett.* **2011**, *13*, 600. (f) Melchionna, M.; Nieger, M.; Helaja, J. *Chem.—Eur. J.* **2010**, *16*, 8262. (g) Jurberg, I. D.; Odabachian, Y.; Gagosz, F. *J. Am. Chem. Soc.* **2010**, *132*, 3543. (h) Kang, Y. K.; Kim, S. M.; Kim, D. Y. *J. Am. Chem. Soc.* **2010**, *132*, 11847. For a recent review, see (i) Haibach, M. C.; Seidel, D. *Angew. Chem., Int. Ed.* **2014**, *53*, 5010.

(27) Roth, W. R.; Konig, J. *Liebig's Ann. Chem.* **1966**, *699*, 24.

(28) (a) Heimgartner, H.; Zsindely, J.; Hansen, H.-J.; Schmid, H. *Helv. Chim. Acta* **1973**, *56*, 2924. (b) For a recent mechanism study, see Alajarin, M.; Bonillo, B.; Marin-Luna, M.; Sanchez-Andrada, P.; Vidal, A. *Chem.—Eur. J.* **2013**, *19*, 16093.

(29) Hammond, G. S. *J. Am. Chem. Soc.* **1955**, *77*, 334.

(30) (a) Rzepa, H. S.; Wentrup, C. *J. Org. Chem.* **2013**, *78*, 7565. (b) Kraka, E.; Cremer, D. *Acc. Chem. Res.* **2010**, *43*, 591.

(31) The [1,2]-H shift could be assisted by a trace amount of water or other proton source. To test this, we carried out the cycloisomerization of **3-MeOC₆H₄** catalyzed by PtCl₂ in the presence of D₂O and CD₃OD (in ref 17f, there are discussions of the effects of water and methanol). In both cases, there were no D atom incorporation in the final products, suggesting that the present [1,2]-H shift take place intramolecularly (see the Experimental Section for details). Previously, we have shown that water-catalyzed [1,2]-H shift in Au system needed the help of some substituent as a handle, which can form complex with water through hydrogen bond. In the present system, no such functional group is available in the substrate and water or methanol-catalyzed [1,2]-H shift is not operative. In addition, under heating at 120 °C, D₂O or CD₃OD could evaporate from the reaction system and cannot participate in the reaction. Also experiments from Yamamoto, Chatani, and He using D-substituted substrate supported that D atoms at C2 and C3 positions of the final

cyclization products came from the organyl benzylic position (see refs 4 6, and 7). For the discussion of water-catalyzed [1,2]-H shift, see:

(a) Shi, F.-Q.; Li, X.; Xia, Y.; Zhang, L.; Yu, Z.-X. *J. Am. Chem. Soc.* **2007**, *129*, 15503. For water-catalyzed [1,2]-proton shift processes supported by experiments and DFT calculations, see: (b) Xia, Y.; Liang, Y.; Chen, Y.; Wang, M.; Jiao, L.; Huang, F.; Liu, S.; Li, Y.; Yu, Z.-X. *J. Am. Chem. Soc.* **2007**, *129*, 3470. (c) Liang, Y.; Liu, S.; Xia, Y.; Li, Y.; Yu, Z.-X. *Chem.—Eur. J.* **2008**, *14*, 4361. (d) Liang, Y.; Liu, S.; Yu, Z.-X. *Synlett* **2009**, 905.

(32) (a) Wagner, P. J.; Giri, B. P.; Scaiano, J. C.; Ward, D. L.; Gabe, E.; Lee, F. L. *J. Am. Chem. Soc.* **1985**, *107*, 5483. (b) Shchukin, A. O.; Vasil'ev, A. V. *Russ. J. Org. Chem.* **2007**, *43*, 784.

(33) When we repeated this reaction, sometimes the substrate cannot be consumed completely and the reaction gave a mixture of substrate and two products (conversion: 85%, brsm: 49%, ratio of **3P-C₆H₅**/**3P'-C₆H₅** = 3.0:1; conversion 45%, brsm: 48%, ratio of **3P-C₆H₅**/**3P'-C₆H₅** = 2.8:1). We speculated that the quality of the used PtCl₂ catalyst could be a factor affecting the reaction outcomes.

(34) Zeng, X.; Ilies, L.; Nakamura, E. *J. Am. Chem. Soc.* **2011**, *133*, 17638.